MODESTUM
OPEN ACCESS

Eurasian Journal of Analytical Chemistry, 2018, 13(5), em42
ISSN:1306-3057
Research Paper https://doi.org/10.29333/ejac/93424

Discovery Potent of Bagasse (CMC-L-Phe) As Bioactive Material Based on DFT Calculations

Ahmed A. El-Henawy [1*], Altaf H. Basta [2*], Houssni El-Saied [2], Essam H. Abdel-Shakour [3], Mohamed S. Hasanin [2], Hussein H. El-Sheikh [3]

[1] Chemistry Department, Faculty of Science, Al-Azhar University, Cairo, EGYPT
[2] Cellulose & Paper Dept., National Research Centre, El-Buhouth St., Dokki-12622, Cairo, EGYPT
[3] Botany and Microbiology Department, Faculty of Science, Al-Azhar University, Cairo, EGYPT

Received 14 March 2018 ▪ Revised 25 May 2018 ▪ Accepted 13 June 2018

ABSTRACT

This present work deals with evaluating the safety application of synthesizing nano-CMC-L-Phe bioactive compound, as drug discovery application, using DFT theories. In this respect, the stereochemistry studies as well as geometrical optimization of ligand at density functional theory (DFT), using DFT\B3LYP with 6- 31G* level of theory calculation of frontier molecular orbitals (FMOs) were carried out. These calculations were performed for studying the stability and reactivity of ligand, heat formation, dipole moment, polarizability, thermodynamic parameters, calculated global, local chemical reactivity to give better understanding; as well as structure-property relationships (SPR) based on electronic structure of the CMC-Phe. The global and local chemical reactivity were examined for synthesized biopolymer, which showed the L-form more reactive against surrounding biological media than D-form. The ADMET profile was calculated in silico, the pharmacokinetic parameters of the ligand showed the promising futures for drug application. The docking study was suggested that, the CMC-L-Phe have a good binding affinity, and interacted with FAK active site to form stable complex, this is evident the ligand is suitable FAK inhibitor.

Keywords: amino acid, nano-cellulose derivatives, Bagasse CMC, stereochemistry and DFT

INTRODUCTION

Cellulose acetate (CA) and carboxymethyl cellulose (CMC) regard the most chemistry market cellulose derivatives. Where, they have wide range of applications, e.g., RO-membranes for water desalination, metal absorbents, stabilizing agents and paper additive [1-5]. Moreover, CMC has been applied in tissue engineering of cartilage [6-8], for treating dry eye after phacoemulsification [9], as filler in tablet with active ingredients [10], as well as additive to increase the drug bioavailability and releasing [11], Mixtures of amino acid and CMC, have been used to obtain zero-order releases of drugs, with water as the releasing medium [12], or simulated gastric media [9].The literature reported different methods to evaluate the bioactive compound, e.g., via biological, using antimicrobial plate diffusion method [13-15], as well as anti-tumor test, using the microculture tetrazolium Assay (MTT) [16, 17] Where, cell viability was assessed and cytotoxic index IC_{50} was calculated. Moreover, computational programs, e.g., the TarFishDock, TargetHunter, Similarity Ensemble Approach ChemMapper and HitPick methods are reported, to give us the information's about the molecular structure [18-24]. The Discrete Fourier Transform (DFT) regards the most benefit discrete transform, used in many practical applications, moreover to efficiently solve partial differential equations, and convolutions or multiplying large integers [25]. On the other hand, pharmacokinetic information is required to optimize the pharmacodynamic response [26], and consequently indicates the bioavailability of drug (percentage of the administered drug which arrives in the central compartment).

✉ elhenawy_sci@hotmail.com **(*Correspondence)**
✉ altaf_halim@yahoo.com altaf_basta2004@yahoo.com **(*Correspondence)** ✉ houssni_nrc@yahoo.com
✉ essam_hussain@hotmail.com ✉ sido_sci@yahoo.com ✉ elshiekh20152016@yahoo.com

Despite most of literatures deal with approaches to cancer treatment are based on chitin and chitosan derivatives [27-30], however till now additional innovative approaches are required to design the low cost drugs for treating the anticancer, together with reducing the toxicity and improving the rapeutic indices. In our previous work, we succeeded in synthesizing CMC-based biological active agent, in nano-size structure, from modifying the carboxymethyl cellulose (market) with L-phenylalanine (L-Phe) [29]. Bagasse is promising cellulosic material available in Egypt and other many countries, as non-wood source, therefore, in continuation and supporting the safety application of this novel nano compound in pharmaceutical purpose, in this present work the performance of bagasse-CMC-L-Phe compound, as bioactive, is assessed beside its ability to demonstrate and predict safety drug discovery applications and rationalizing drug side effects. For this purpose, we study some quantum theories, and highlight on structure geometry, moreover we shed light on the geometries-electronic properties as well as quantum structure-property relationship.

MATERIALS AND METHODS

Conjugate compound*:* Carboxymethyl cellulose (CMC) and L-phenylalanine (L-Phe) were used as materials for the synthesis bioactive conjugate compound. CMC was prepared from α-cellulose extracted bagasse; according to method described in Ref 28. Its purity and DS are 99% and 0.92, respectively. While, the ***L-Phe*** was purchased from Oxford, India, with specifications (purity 99.5 %; other amino acid content, 0.01 %). The synthesis approach was carried out under recommended conditions reported at our previous work [29]. In this method CMC and L-Phe were reacted (in ratio 1.5) by condensation reaction at temperature 250 ^{o}C for 1.5 hr.

Morphological Characterization of the synthesized bagasse***-CMC-L-phe*** in nano form was carried out by using transmission electron microscopy, of type QUANTA FEG250, Japan **(**System running at 200 keV). While, the evidence of modification of CMC was performed by Infrared spectra, using Jasco FT/IR, Nicolet, and Model 670. The samples were mixed with KBr and pressed as tablet. The bands were recorded in the region from 4000 to 400 cm^{-1} with Deuterated Triglycine Sulfate (DTGS).

Computational Model

- The Quantum chemical computations were performed with the Becke3-Lee-Yang-parr (B3LYP) level, 6-311G*, basis as implement in Gaussian 09W program package [31] as implemented in MOE package [32]. The optimization Geometry for molecular structure was carried out, for improving knowledge of chemical structure.
- The thermodynamic functions as, entropy, Zero-Point Vibrational Energies (ZPVE) at 298.15K and (1 atm) pressure, entropies (S^0) and enthalpy changes (ΔH^0), for the compound were evaluated by the theoretical harmonic frequencies obtained from B3LYP/6-311G* method. The dipole moments and polarizability were calculated against to *X, Y* and Ztrace of the polarizability tensor, which is responsible to an external electric field at zero frequency; as following equations:

$$D = (D^2x + D^2y + D^2z) \quad (1)$$

$$The\ isotropic\ polarizability\ \beta = 1/3\ (\beta^2_{xx} + \beta^2_{yy} + \beta^2_{zz}) \quad (2)$$

- The following equation (BDE = $H°_{\bullet} + H°_{H} - H°_{\pm}$) was used for estimating enthalpyof bond dissociation (BDE) values" where; $H°_{\bullet}$, $H°_{H}$, $H°_{\pm}$, the enthalpy of the radical generated by H releasing, H-atom, and the parent molecule, respectively. The adiabatic IP values were calculated according to the equation IP = I^{+} - $I^{\pm}$, where I^{+} (parent molecule), $I^{\pm}$ (cation radical generated after electron transfer).
- Global chemical reactivity descriptors for molecules have been computed, as S; softness (measures stability of molecules and chemical reactivity with direct proportional) [33], η; hardness (reciprocal of softness), μ; chemical potential, χ; electronegativity (strength atom for attracting electrons to itself, ω; electrophilicity (measuring lowering energy due to maximal flowing electron between donor and acceptor) [34-38], μ−; electron donating chemical potentials, and μ+; electro accepting processes, ability powers for ω−; electro donating, and ω+; electro accepting. These expressions are in terms of the I; first ionization potential (the difference of the total electronic energy when an electron is removed (N − 1) from the neutral molecule with N electrons at a constant external electron potential), and the A; electron affinity (υ(r), which calculated under the same conditions when an electron is added (N + 1) [35], Electrophilicity index (ωi):

$$\eta = \frac{1}{2}\left(\frac{\partial^2 E}{\partial^2 N^2}\right)_{V(\acute{r})} = \frac{1}{2}\left(\frac{\partial \mu}{\partial N^2}\right)_{V(\acute{r})} \quad (3)$$

$$\mu = \left[\frac{\partial E}{\partial N}\right]_{V(\acute{r})} \quad (4)$$

$$\chi = -\mu = -\left[\frac{\partial E}{\partial N}\right]_{V(\acute{r})} \quad (5)$$

$$S = \frac{1}{\eta} \quad (6)$$

$$\omega = \frac{\mu^2}{2\eta} \quad (7)$$

$$\mu^- = \_¼(3I + A) \quad (8)$$

$$\mu^+ = \_¼(I + 3A) \quad (9)$$

$$\omega^- = -(3I + A)^2 \,/\, 16(I - A) \quad (10)$$

$$\omega^+ = (3I + A)^2 \,/\, 16(I - A) \quad (11)$$

$$w_i = \mu/2\acute{\eta} \quad (12)$$

Taking into account, the expression $\omega^{\pm}$; is net electrophilicity ($\omega^{\pm}=\omega^{+}+\omega^{-}$), it can be expressed as the measurement of the electron accepting power relative to its electron donating power [34], ***E*** is electronic energy, and ***υ(r)*** is external potential of an N-electron system.

- Energy back donation is equational expressed when a molecule received a specific quantity of charges ΔN^+ , associated with the energy change ΔE^+ as [35]:

$$\Delta E += \mu P + \Delta N^+ + 1/2\,\eta\,(\Delta N^+)^2 \quad (13)$$

When a molecule back donates a specific quantity of charges ΔN^- associated with the energy change ΔE^- as:

$$\Delta E -= \mu P^- \Delta N^- + 1/2\,\eta\,(\Delta N^-)^2 \quad (14)$$

The Sum of (13) and (14) equations to give amount of charges received: $\Delta N^- = -\Delta N^+$.

$$\Delta E_{bd} = \Delta E^+ + \Delta E^- = (\mu p^+ - \mu P^-) - \Delta N^+ + \eta\,(\Delta N^+)^2 \quad (15)$$

The total energy change is minimum with respect to ΔN^+ and implies that

$$\Delta N^+ = -(\mu P^+ + \mu P^-) \,/\, 2\,\eta \quad (16)$$

$$\Delta_{ET} = -(\mu P^+ - \mu P^-)^2 \quad (17)$$

- The site selectivity of a chemical system cannot be studied by using the global descriptors of reactivity. Thus, appropriate local descriptors need to be defined. The HSAB principle has been used in a local sense in terms of DFT concepts [36], such as the Fukui function ***f(r),*** which described the reactivity of a specific atom in a molecule. It is necessary to condense the values of ***f(r)*** around each atomic site into a single value that characterizes the atomic contribution in a molecule. The atom ***k*** in a molecule, depending upon the type of electron transfer. Three kinds of condensed Fukui function of the atom ***k*** can be obtained. According to Ref. 36 the sites which have highest values of Fukui Function ***f(r)*** is more reactive center in chemical species. The Fukui function is defined as:

$$F(r) = (\delta\sigma/\delta\gamma)_N = (\rho(r)/\delta N)_\gamma \quad (18)$$

where σ (electronic chemical potential), N (number of electrons), p (corresponds to the electron density) and γ(external potential exerted by the nucleus). The Fukui function is; a local reactivity descriptor that indicates the preferred regions, when modifying the number of electrons at chemical partials and changing the electron density. Therefore, it indicates the propensity of the electronic density to deform at a given position upon accepting or donating electrons [36-39]. The second formula for $f(r)$, $(\delta\sigma/\delta\gamma)_N$ is a quantity involving the electron density of the atoms or in its frontier valence regions. For an N-electron system, independent calculations have been made on (N-1), (N) and (N+1) electronic system with the same molecular geometry. Various population schemes yield $_{qk}$(N-1),$_{qk}$(N) and $_{qk}$(N+1) for all the atoms, then these values are substituted in the following equations and obtained the corresponding Fukui function values for$F_J^{\pm}, F_J^{-} and F_J^{0}$. In a finite-difference approximation, the values are calculated as:

$$For\ nucleophilic\ attack\ F_k^{\pm}(r) = (\rho(r)/\delta N)(_{\gamma}^{\pm}) = \left[p_{N+1}(r) - p_N(r)\right] = [qk\,(N+1) - qk\,(N)] \quad (19)$$

$$For\ electrophilic\ attack\ F_k^{-}(r) = (\rho(r)/\delta N)_{\gamma}^{-} = \left[p_N(r) - p_{N-1}(r)\right] = [qk\,(N) - qk\,(N-1)] \quad (20)$$

$$For\ radical\ attack\ F_k^{0}(r) = (\rho(r)/\delta N)(_{\gamma}^{0}) = 1/2\left[p_{N+1}(r) - p_{N-1}(r)\right] = 1/2[qk\,(N+1) - qk\,(N-1)] \quad (21)$$

- The local softness contains the same information as the Fukui unction (i.e., the sensitivity of the chemical potential of a system to a local external potential), as well as additional information about the molecular softness. The local softness and electrophilicity (philicity) indices are calculated using Eqs. (22) and (23), given respectively as:

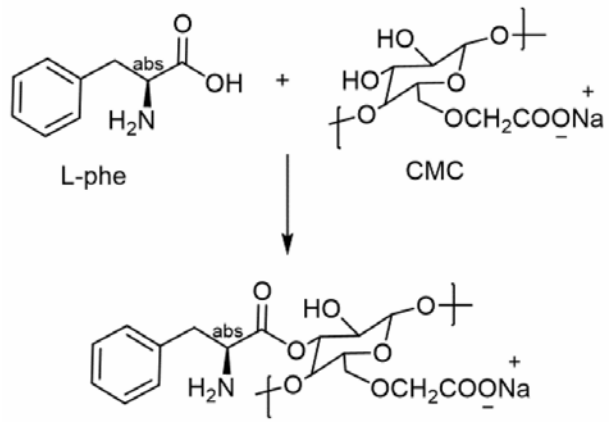

Figure 1. Synthesis of bioactive CMC-Phe polymer unit

$$S_k^{\pm} = SF_k^{\pm}, S_k^{-} = SF_k^{-}, S_k^{0} = SF_k^{0} \quad (22)$$

$$\omega_k^{\pm} = \omega F_k^{\pm}, \omega_k^{-} = \omega F_k^{-}, \omega_k^{0} = \omega F_k^{0} \quad (23)$$

where "+" (nucleophilic)," −" (electrophilic) and "0" (radical). The intra- and inter-molecular reactivity descriptors can be elucidate by relative nucleophilicity $S_k^-/S_K^{\pm}$ and electrophilicity $S_K^{\pm}/S_k^-$, this descriptors have been helpful tools for studding nucleophilic and electrophilic reactions [40-42].

- The changes of the electronic density when system is accepts electrons, ρ, are associated to the k_{th} atom, $\Delta\rho_K^{Elec}$ is expressed by

$$\Delta\rho_k^{Elec} = -\frac{\mu^+}{\eta} f_k^+ + \frac{1}{2}\left(\frac{\mu^+}{\eta}\right)^2 (f_k^+ - f_k^-) \quad (24)$$

The changes of the electronic density when system is donate electrons, ρ, are associated to the *kth* atom, $\Delta\rho_K^{Nuc}$ is expressed by

$$\Delta\rho_k^{Nuc} = \frac{\mu^-}{\eta} f_k^- + \frac{1}{2}\left(\frac{\mu^-}{\eta}\right)^2 (f_k^+ - f_k^-) \quad (25)$$

Stepwise Docking Method

The 3D crystal structure of FAK was obtained from Protein Data Bank (PDB ID: 4K9Y) [43] and 4K9Y has a good resolution (2 Å) and attached co-crystallized inhibitors are used to identify the active site. The crystal structures of the (4K9Y**1**) as reference inhibitor molecule is used. Water and inhibitor molecule is removed, together with added hydrogen atoms. The parameters and charges are assigned with MMFF94x force field. Alpha-site spheres are generated using the site finder module of MOE. The optimized 3D structures of molecules were subjected to generate different poses of ligands using triangular matcher placement method, which generating poses by aligning ligand triplets of atoms on triplets of alpha spheres representing in the receptor site points, a random triplet of alpha sphere centers is used to determine the pose during each iteration. The pose generated is rescored using London ***dG*** scoring function. The poses generated are refined with MMFF94x force field; also, the solvation effects are treated. The Born solvation model (GB/VI) is used to calculate the final energy, and the finally assigned poses were assigned a score based on the free energy in kJ/mol.

RESULTS AND DISCUSSION

The synthesized bagasse- ***CMC-L-Phe***, with nitrogen content 1.4%, is illustrated in **Figure 1**; while **Figure 2** shows the stero-isomer forms and TEM. The TEM photograph (**Figure 3.a**) confirms the bagasse conjugate is synthesized in nano-particles (between 50 – 100 nm). The insolubility behavior of this compound in water is strong evidence for the formation of this new compound, due to excellent solubility of the two reactants.

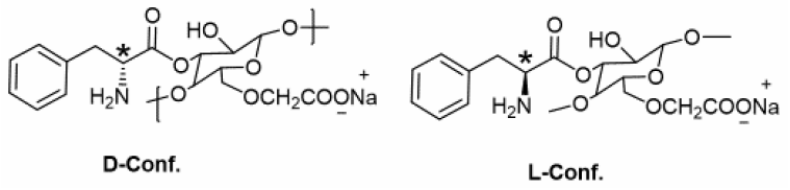

Figure 2. Stero isomer form of CMC-Phe polymer unit

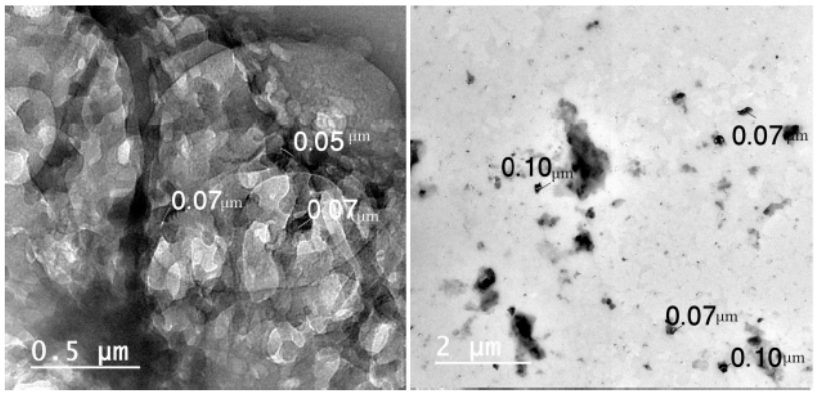

(a)

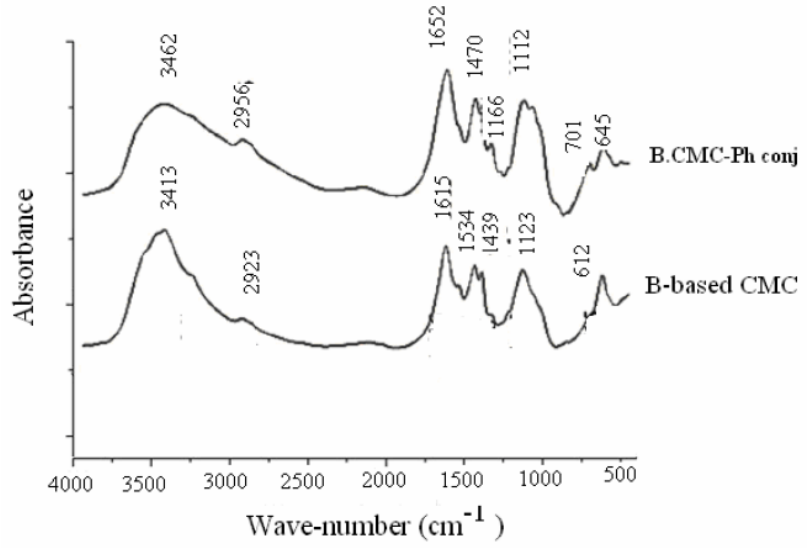

(b)

Figure 3. a) TEM of bagasse-CMC conjugate b) FT-IR spectra of bagasse –CMC and bagasse-CMC conjugate

With regard to evidence the functionalization of CMC by ***L-Phe***, we previously used FT-IR spectra. **Figure 3.b** shows the IR spectrum of ***bagasse -CMC-L-Phe*** in comparison with bagasse-CMC. It is clear that, conjugating the CMC with amino acid leads to blue shift the band of stretching vibration of OH groups from 3412 cm^{-1} to 3462 $cm.^{-1}$ Also the band related to C=O at 1616 cm^{-1} is shifted to 1652 cm^{-1} together with the appearance of noising bands at 1046 $cm.^{-1}$ This confirms that the free unsubstituted hydroxyl groups of CMC (2ry alcohol) are condensed with COOH group included L-phenylalanine and consequently may be lead to liberate the hydrogen bonded of 2ry hydroxyl, during synthesis processes.

Molecular Modeling

In attempting to accomplish good understanding of the most stable stereoisomer polymer forms (**Figure 4**), the conformational analysis of the studied polymer ***CMC-L-Phe*** is performed using density function theory (Gaussian 09 package), as implemented in MOE2015. The geometrical optimization and computed molecular parameters are carried out using B3LYP with 6-311G* basis set.

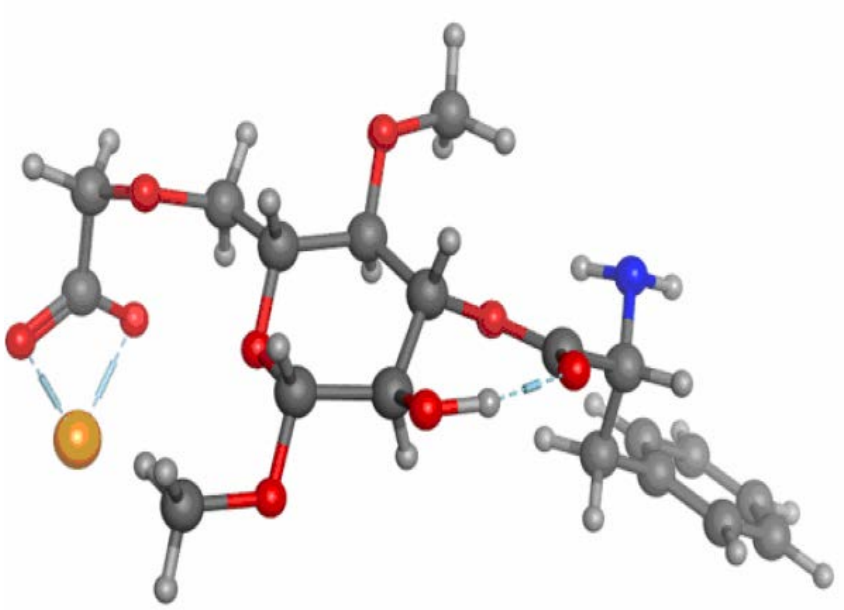

Figure 4. Ball and stick rendering for the most stable steroisomer ***CMC-L Phe*** with intramolecular hydrogen bond of the ligand, as calculated DFT molecular orbital with **B3LYP/6-311G***

Table 1. Calculated energetic, thermodynamic and global reactivity parameters for CMC-Pheat DFT with a B3LYP\6-31G* Basics sets

			L						***D***		
E	*-1006619.6*	α	*2443.958*	*χ*	*-4.304*	*E*	*-1006619.6*	α	*618.99*	*χ*	*-4.258*
Eele	*-35.646*	β	*2082.63*	*I*	*8.919*	*Eele*	*-35.646*	β	*814.652*	*I*	*8.474*
HF	*-443.138*	β_{xx}	*175.119*	*IP*	*-4.119*	*HF*	*-436.216*	β_{xx}	*2064.240*	*IP*	*-3.675*
Eb	*-1623.32*	β_{xy}	*1037.88616*	*A*	*0.133*	*Eb*	*-1486.92*	β_{xy}	*1311.723*	*A*	*0.403*
ZPE	*281.97*	β_{yy}	*5394.63258*	μ^+	*-2.218*	*ZPE*	*259.27*	β_{yy}	*269.166*	μ^+	*-1.927*
H°	*1.544*	β_{yz}	*1748.03688*	μ^-	*-6.389*	*H°*	*1.062*	β_{yz}	*0.0369*	μ^-	*-6.588*
G°	*1.47*	β_{zz}	*185.28746*	*μ*	*4.304*	*G°*	*0.991*	β_{zz}	*61.805*	*μ*	*4.258*
S°	*626.15*	β_{zx}	*707.17533*	ω^-	*4.894*	*S°*	*606.25*	β_{zx}	*0.0366*	ω^-	*4.656*
CV°	*320.21*	*BDE*	*-108.3*	ω^+	*1.699*	*CV°*	*278.75*	*BDE*	*-112.667*	ω^+	*1.362*
Vm	*418.25*	*HOMO*	*-8.919*	ω^{+-}	*6.593*	*Vm*	*404.50*	*HOMO*	*-8.474*	ω^{+-}	*6.0191*
D	*-0.917*	*LUMO*	*0.403*	ω_i	*0.516*	*D*	*-3.264*	*LUMO*	*-0.133*	ω_i	*0.416*
DX	*-2.125*	*ΔG*	*8.341*	ΔN_{max}	*-0.516*	*Dx*	*-0.713*	*ΔG*	*8.341*	ΔN_{max}	*-0.4567*
Dy	*-0.210*	*η*	*4.17*	ΔE_{bd}	*-1.165*	*Dy*	*-0.754*	*η*	*4.66*	ΔE_{bd}	*-1.042*
Dz	*1.418*	*S*	*0.2397*			*Dz*	*-1.796*	*S*	*0.21*		

E**: The total energy (kcal/mol),**E-ele**: electrostatic energy (kcal/mol), **HF**: heat of formation (kcal/mol),* **Eb:** *binding energy,* **ZPE:** *zero-point vibrational energies(kj/mol),,* **H°:** *Enthalpy (kj/mol),* **G°:** *Gibbs free energy (kj/mol),* **S°:** *Entropy (kj/mol),* **Cv°**: *Constant volume molar heat capacity,* **MV:** *Molecular volume A^2,* **D**: *dipole moment (Deby),* **α:** *polarizability;* **β:** *anisotropic polarizability,* **BDE:** *Bond dissociation energy,* **HOMO**: *Highest Occupied Molecular Orbital (eV),* **LUMO**: *Lowest Occupied Molecular Orbital (eV),* **ΔG**: *difference between HOMO and LUMO energy levels(eV),* **η:** *Hardness(eV),* **S:** *Softness(eV),* **χ :** *Electronegativity (eV),I:** *first ionization potential,* **IP:** *Ionization potential,* **A;** electron affinity**; μ^+:** *electron accepting chemical potentials,* **μ^-:** *electron donating chemical potentials,* **μ:** *chemical potential(eV),* **ω^+:** electron accepting **, ω^-:** electrodonating power; **ω^+ ω^-: :Electrophilicity (eV); ω_i :** *electrophilicity* index; **ω**, **ΔE_{bd}:** Back-donation energy, **ΔN_{max}:** maximum number of electrons transfer;

Molecular Geometry

The synthesized polymer has a chiral C atom (*), thus, the two stereoisomer forms may be possible existence (**Figure 2**). Experimentally elucidation of the preferred stereoisomer for ligand structure is complicated. The total energy have been used to investigate the most stable form for a prepared polymer, and showed that, ***CMC-L-Phe*** form is more stable than CMC-***D-Phe*** (**Figure 4**, **Table 1**).

- The ***CMC-L-Phe*** is stabilized by an arrangement of phenyl ring of amino acid perpendicular mode with pyranose ring; the distance of O-Na is lengthening in L form than D- Form due to free rotation of pyranose ring around axes. The bond between Carbonyl groups C17-O27 and C13-O24 are 1.18 and 1.17 °A for L and D forms, respectively. The lengthening distance between two carbonyl groups may be explained by adjacent electronegative oxygen atoms, which withdrawing electrons of C13 and releasing electron to O24, with

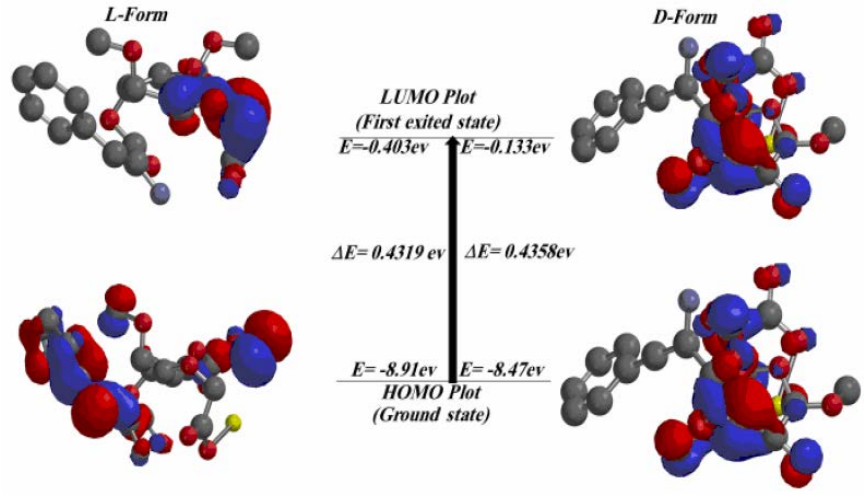

Figure 5. Plotting of the frontier molecular orbital for ***CMC-D/L-Phe***

lengthening bond distance. The intra-molecular hydrogen bond formation is between $O_{27}\cdots H_{32}$ (1.9°A), and the bond angles of C17-C19-O_{27} is larger than H31-O5-C3 (179° and 79 °), this is ascribed to inter-molecular interaction (**Sup. Figure 3** and **4**, in **supplementary data**).

- The computed vibrational frequencies (**Sup. Figure 2** in **supplementary data**) and molecular parameters of the target compounds have been performed. The computed vibration values are agreement with slightly division comparable with our experimental results (**Figure 1**). The deviation values between the experimental and calculated, may be due to the performance theoretical calculations in the gaseous state for the single molecule without intra-molecular interactions, in contrary, the experimental values have been recorded in the presence of intermolecular interactions.

Transfer Mechanism

Two serious mechanisms may be parallel occurred for bioactive molecules in chemical or biological system; one: the H-atom transfer mechanism (A + BOH → AH + BO•), and the other is the electron transfer mechanism (A + BOH → A + BOH^+). The activity of BOH molecule is related to radical stability ($BO^•$), which estimated by H-bond, conjugation, and resonance effects. The reactivity of an (BOH) is determined by calculating the bond dissociation enthalpy (BDE) for hydroxyl group. Thus, the generated cation radical from the electron transfer must be stable; hence, the antimicrobial potency can be exhibited by the adiabatic ionization potential (IP). Decreasing I, IP and BDE values are expected to enhancement antimicrobial activity. The ***CMC-L-Phe*** showed decreasing in I, IP and BDE values than ***CMC-D-Phe***, this may be suggested the enhancement activity of L form than D-form derived from CMC (**Table 1**).

Frontier Orbital Analysis

The frontier molecular orbital's HOMO and LUMO are estimated the interaction pathway between the molecule and receptor. The E_{HOMO}, is exhibited the ability electron donating of the molecule; while E_{LUMO} is ability electron gaining of a molecule [43]. The "simple Hückel Molecular Orbital theory (SHMO)" is used to study the frontier orbital gap; which exhibited the reactivity and stability of the molecule [43-45]. The (HOMOs) and (LUMOs) are studied in the S0, which suggested the delocalization HOMOs around pyranose and phenyl rings; as well as LUMO is localized in carboxylate group for L- and D forms (**Figure 5**). The HOMO energy for ***CMC-L-Phe***is is greater than ***CMC-D-Phe***, and vise verse for LUMO energies (**Table 1**, **Figure 5**). The energy gap for ***CMC-L-Phe*** is smaller than for the ***CMC-D-Phe***, which indicated favorable ability interaction with FAK receptor.

Thermodynamic Properties

The 2nd law of thermodynamics parameters has been inducing helpful tools for estimation the activity direction of biomolecule. The total dipole moment (D), and related thermodynamic properties (mean polarizability(***α***), and anisotropy polarizability(***β***)), which showing the interacting power of the molecules with media, in case of L isomer are higher than D-isomer. Where, the polarizability of L isomer is -0.97*Deby*; while for D isomer is -3.264*Deby*. The anisotropic and polarizability of ***CMC-L-Phe are*** *approximately* ~ 2.5 and 4 times greater than ***CMC-D-Phe,*** respectively (**Table 1**). This leads to increase its ability of interaction with the surrounding environments. Thus, a

Table 2. Minimal inhibitory concentration of the compound on the tested strains Bacteria and fungi

Conc. (µg/ml)	Clear zone diameter (mm)								
	Bacteria					Fungi			
	B.subtilis (NCID-3610)	*S. aureus (NCTC-7447)*	*P. aeruginosa (NCID-9016)*	*E.coli (NCTC-10416)*	*Candida albicans (NCCLS 11)*	*Aspergillus awamori (ATCC22342)*	*Cunninghamella elegans (ATCC 36112)*	*Aspergillus niger (ATCC 22342)*	*Penicilliumsp. (NRRL 1889)*
20.0	5.00	7.00	0.00	6.00	4.00	3.00	5.00	0.00	0.00
10.0	0.00	0.00	0.00	0.00	0.00	0.00	0.00	0.00	0.00
5.00	0.00	0.00	0.00	0.00	0.00	0.00	0.00	0.00	0.00
2.50	0.00	0.00	0.00	0.00	0.00	0.00	0.00	0.00	0.00
1.25	0.00	0.00	0.00	0.00	0.00	0.00	0.00	0.00	0.00
0.00	0.00	0.00	0.00	0.00	0.00	0.00	0.00	0.00	0.00

CMC-L-Phe molecule is a promising structure for formation strong interaction with receptor of microorganism (FAK).

The molecular volume (MV) has been the connection image between the tested polymer and the microbial surface [47]. The observed higher volume (~418 A^2), with stronger binding energy (1623.32 *kcal/mol)* for L-form it promotes the chance for stability binding interaction with receptor surface than D form, which showed volume (404.50A^2) with binding energy (1486.92 *kcal/mol)* (**Table 1**). Generally, all calculated thermodynamic parameters for the ***CMC-L-Phe***are are greater than ***CMC-D-Phe*** (**Table 1**). These parameters demonstrated that, the ***CMC-L-Phe*** is higher chance for biological application.

Chemical Reactivity

Global reactivity descriptors

- The maximum hardness principle (***MHP***) is qualitative helpful technique for studding system stability, which revealed that, the system have been more stable if it has low hardness properties. Thus, the molecular stability for synthesized polymer has been analyzed based on this DFT basic. The global reactivity properties which are calculated and registered in (**Table 1**); are ***HOMO*** *(eV),* ***LUMO*** *(eV),* ***ΔG*** *(eV),* ***η:*** *(eV),* ***S:*** *(eV),* ***χ :*** *(eV),* **A;;** ΔE_{bd}**:** Back-donation energy;μ^+**:**electron accepting chemical potentials**,** μ^-**:** electron donating chemical potentials**,** ***μ:*** chemical potential*(eV),* ω^+**:** electron accepting **,** ω^-**:** electrodonating power; ***ω***:Electrophilicity *(eV),* ΔN_{max}**:** and maximum number of electrons transfer. The tabulated data (**Table 1**) reveal that, the ***L-***polymer structure has preferred than ***D-*** form.
- The ***CMC-L-Phe*** has smaller hardness (4.17 ev) and larger value for softness (2.39 ev), which indicate the ***CMC-L-Phe*** is a reactive molecule toward FAK (**Table 1**).
- The negative value of μ− (-2.218, eV) for ***L-*** form is higher than (-1.92 eV) D-form, as well as the value for μ+ (-6.38 eV) is lower than (-6.58 eV) D form, In other hand, the electron donating power ***ω–(***4.89 eV**)** for L-isomer is greater one time than (4.65 eV) D form; while the electron accepting power ***ω+***(1.69) for ***CMC-L-Phe*** is smaller than (1.66 eV) ***CMC-D-Phe***. This data suggested the higher ability of the ***CMC-L-Phe*** molecule for donating electron to environment.
- The calculated ΔN_{max} according to Ref. 47, is another quantum chemical parameter, which referred to a maximum number of electrons transferred in a chemical reaction (**Table 1**). The electrophilicity has been reflected the ability donating electrons to the media [48], the high electrophilicity compound is defined as a Lewis acid (electron-rich). The ***CMC-L-Phe*** is one time more electrophilicity properties than ***CMC-D-Phe,*** which explained by less electronegative atoms ***CMC-L-Phe*** interacted with negative charge located in microbial surface (**Table 1**).
- Energy back donation is the term determines the interaction between compounds and surface of FAK receptor. This term is combined with charge transfer and directly proportional with hardness. It is revealed that, the compound is energetically favored, if η more than zero and ΔE Back-donation less than zero [49]. This observation reveals the greatest interaction efficiency of ***L-***form than ***D-***form (**Table 1**).
- The natural bond orbital (NBO), are computed within full bond orbital analysis at B3LYP/6-311G* G, for the ligand and its complex (**Sup. Figure 5** in **Supplementary material**). The distribution of charges upon the atomic region exhibits that, the formation of donor and acceptor pairs involving the charge transfer in the molecule. In general, the atoms charged with positive charges are; hydrogen, some carbons, nitrogen, and oxygen. Some carbon atoms have negative charges. The O5 is the most negative centers, on contrary, the maximum positive charge for ligand is located in C17.

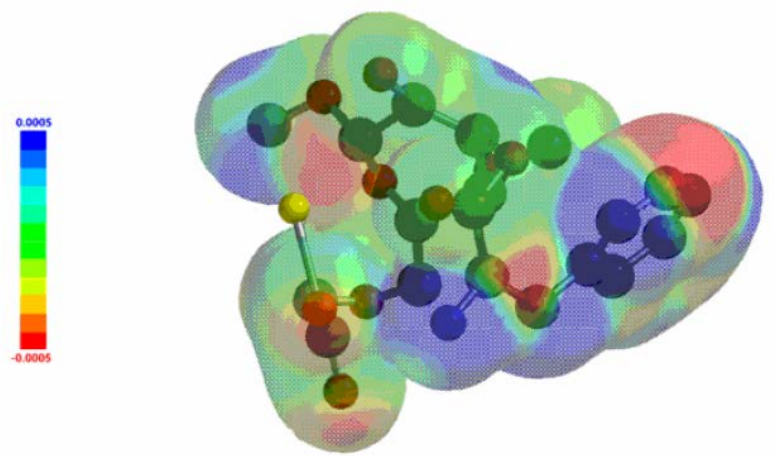

Figure 6. ESP mapping for the most stable stereoisomer form of the ligand as calculated DFT molecular orbital with B3LYP/6-311G*

Local reactivity and intermolecular interaction

- The global reactivity cannot be satisfying for explain intermolecular interaction, the local descriptors, using Fukui function, can be used for understanding reactivity site of bio molecule [50]. The electrophilic, nucleophilic and radical attack have been calculated to help us understanding the intermolecular hydrogen bonding interaction. The site with higher" ***f(r)***" Fukui parameter, is larger reactivity site in chemical species and vice versa. The values of electronic density distribution, electrophilicity and softness affect with both values of; the dual descriptor and Fukui function. The site with high positive values of $\Delta\rho_K^{Elec}$ is most electrophilic region, and a nucleophilic attack may be took place. In contrary, increasing the negative value of $\Delta\rho_K^{Nuc}$ in specific zone, indicating high nucleophilic in this site and electrophilic attack may occur. The F^{+}, F^{-},F^{0} Fukui functions and; F^{2} dual descriptor, ω^{+},ω^{-},$\omega^{\pm}$ electrophilicity and S^{+},S^{-},$S^{\pm}$ local softness, S^{-}/S^{+} relative nucleophilicity and S^{+}/S^{-}electrophilicity are calculated using DFT theory (**Sup. Table 1** and **2** in **supplementary material**). The C19 is the best sites for a nucleophilic attack with $\Delta\rho_K^{Elec}$=12.39 andS^{-}/S^{+} ***=1.01***, while the electrophile attack take place on O24 (CO of amino acid) with $\Delta\rho_K^{Nuc}$ =0.76 and S^{+}/S^{-}***=0.882***, which provided that, O atom located in outside the plane of the aromatic ring, and due to localize lone pairs of electrons on the unsaturated system the basicity increased..
- The electrostatic potentials (ESP) mapped of ***CMC-L-Phe*** are identified the characteristic electronic and conformational likeness. The pink and blue regions, showed the negatively and positively sites of ESP, respectively. On comparison of the ESP of a ligand with complex, it indicates that, increasing positive charge regions located in the center of coordinating metal in comparison with ligand (**Figure 6**). The charge deformation upon the atoms exhibits the transformation of electrons during formation of donor and acceptor. The charged atoms with positive charges are; hydrogen, some carbon, the nitrogen, the O of N, and some carbon atoms have negative charges. The oxygen atom of carbonyl group is the most negative centers with isovalue (0.0005). On contrary, the maximum positive charge for ligand is located in Na with isovalue (0.0001138), due to attached with a carbonyl group (withdrawing nature). Electrostatic interactions between polymer and the receptor are derived from adsorption stability. The presence of electronegative atoms as NH, OH groups lead to polarity compound, which have a negative charge. The electrostatic attraction between the CMC-L-Phe molecule and the receptor atoms makes the adsorption possible. The hydrophobic nature of amino acid resides in active site receptor, led to lacking ionic character, and hence the overall effect the adsorption energy.

ADMET Factors Profiling

Oral bioavailability has a vital function in discovering the therapeutic bioactive molecules, which neglected in clinical trial, due to the ADMET (absorbance, distributing, metabolic, eliminating and toxicological) parameters. The calculation of ADMET was for bagasse CMC-APP, is also important, and performed as, **i-** (TPSA), which unreferred absorbed molecules if larger than 140 inactive bioavailability [51], **ii-** (% ABS) which was predicted by Zhao *et al*. [52], and **iii-**''Lipinski rule of five'' (**Table 3**). The data show that, the CLogP <5 (factor lipophilicity [53], M.Wt< 500, H - acceptors = 4, H-donors = 1 and molar refractivity values ranged (~118). These evidence that, the

Table 3. Pharmacokinetic parameters for good oral bioavailability, **ADME-Tox** and Docking energy scores (kcal/mol) derived from the MOE of CMC-L-Phe

ADME		***ADME-Tox***			***Docking***
Area	*557.19*	*LogBBB (Blood-brain barrier.)*	*0.016*	*dG*	*-18.0419*
TPSA (Topological Polar Surface Area)	*148.56*	*PPB% (Plasma protein binding)*	*99.63*	*Int.*	*-53.194*
%ABS (Absorption percentage)	*91.4*	*LD50 rat/mouse(mg kg-1, oral)*	*250/590*	*H.B.*	*-10.285*
Vol. (Volume (A3)	*355.97*	*LD50 rat/mouse(mg kg-1, intraperitoneal)*	*300/360*		
Logp (Calculated lipophilicity)	*1.55*	*LD50 mouse(mg kg-1, intravenous)*	*20*		
HBD (Number of hydrogen)	*1*	*LD50 mouse(mg kg-1, subcutaneous)*	*520*		
HBA (Number of hydrogen bond acceptor)	*5*	*Ames test (genotoxicity, %)*	*0566*		
V (Number of violation from Lipinski's rule of five)	*0*	*Prob. of blood effect*	*0.42*		
mr (Molar Refractivity)	*118.02*	*Prob. of cardiovascular System*	*0.92*		
LogS (Solubility parameter)	*-2.00*	*Prob. of gastrointestinal System*	*0.91*		

d.G.: free binding energy of the ligand from a given conformer, Int.: affinity binding energy of hydrogen bond interaction with receptor, H.B.: Hydrogen bonding energy between protein and ligand

Table 4. Interaction between ligand and amino acid residues derived from MOE Docking Tools

Original inhibitor					**CMC-L-Phe**				
Ligand	**Receptor**	**Interaction**	**Distance**	**E (kcal/mol)**	**Ligand**	**Receptor**	**Interaction**	**Distance**	**E (kcal/mol)**
N29 43	*OE2 Glu. 471*	*H-donor*	*2.48*	*-1.5*	*C9*	*OE2 Glu. 471*	*H-donor*	*2.96*	*-2.1*
N32 47	*OE2 Glu. 471*	*H-donor*	*2.65*	*-3.6*	*N-Phe*	*OE2 Glu. 471*	*H-donor*	*2.75*	*-2.2*
N36	*O CYS 502*	*H-donor*	*3.26*	*-1.6*	*N-Phe*	*O CYS 502*	*H-donor*	*3.24*	*-3.8*
N7	*N CYS 502*	*H-acceptor*	*3.06*	*-4.8*	*O29*	*O CYS 502*	*H-acceptor*	*3.21*	*-3.2*

investigated nano- cellulose derivative fulfill Lipinski's rule. The percent absorption of bagasse- CMC-L-Phe is about 91%.

The (ADME-T) algorithm [54, 55] is used for predicting the drug-similarity (**Table 3**). It studying the transport ability of therapeutic agent compounds for transported through the intestinal epithelium. It may be have a strong interacting potency with plasma, through the blood-brain barrier, which necessary led to transport ability drug in the body. In general, No marked health effects in rodent toxicity profiles are observed among its compound ***CMC-L-Phe***. From these data we can suggest that, the compound can be used as a good oral absorption.

Molecular Docking

Focal adhesion kinase (FAK), is also defined as a protein tyrosine kinase 2 (PTK2), which play vital roles in controlling sign from the extracellular matrix (ECM) interceded with two receptors. These receptors are integrins and growing factor (GFR) [56]. FAK is responsible for controlling several cellular transmission information, which regulate several vital processes. [57-59]. The docking examination was performed for give better understanding mechanism of antimicrobial activity for ***CMC-L-Phe***. Molecular docking is the powerful strategy for get a better insight into ligand–receptor interactions. All docking experiment is performed with MOE 2015.10 [31]. In silico, the tested compounds are evaluated using X-ray crystal structures and FAK (ID: 4K9Y) [51], complexes with reference inhibitor. The active site of the enzyme is defined to include residues within a 10.0 Å radius for any inhibitor atoms. MOE scoring function of the most stable docking model for tested compounds is applied to evaluate the binding affinities between the inhibitors with (FAK) active site, (**Table 3**). The minimization in energy is preformed for complexes (inhibitor-active site) with an MMFF94 force field [41,] until the gradient convergence reached to 0.05 kcal/mol. The CMC***-L-Phe*** docked successfully into the FAK active site, and compared with reference inhibitor. The compound ***CMC-L-Phe*** is exhibited highest binding score which reached to -18.04 Kcal/mol (**Table 3**).

The ligand is successfully interacted with the active sites of the FAK, which form two H-bonding interaction viz, Amino acids Glu.471 with good binding free energy (ΔG= -2.1 and -2.2) *kcal/mol*.. Also, the Cys.502 is bonded with ligand by two H-bond with higher binding energy than original ligand (ΔG= -3.8 and -3.2) *kcal/mol,* respectively. The residues ILe428 and Gly505 hold on the phenyl rings of the ligand through alkyl-π interactionsm, with good binding energy. Lys454 is involved in a ionic interaction with the ligand as simulated by MOE (**Table 4**). The ligand is stabilized with itself in binding pocket through, arranged of phenyl ring of amino acid with pyranose ring in coplanar position, which ligand stabilized with binding pocket through arranged L-phy with important active amino acids Lys and Cys in parallel mode (**Figure 7**). The results obtained clearly revealed that, the amino acid residues close to the reference molecule are mostly the same as observed in the tested compound (**Figure 7**). The higher observed binding interaction process, indicated the ligand acts potential inhibitor against FA, this may be explained, the presence of hydrophobic amino acid in the synthesized compounds.

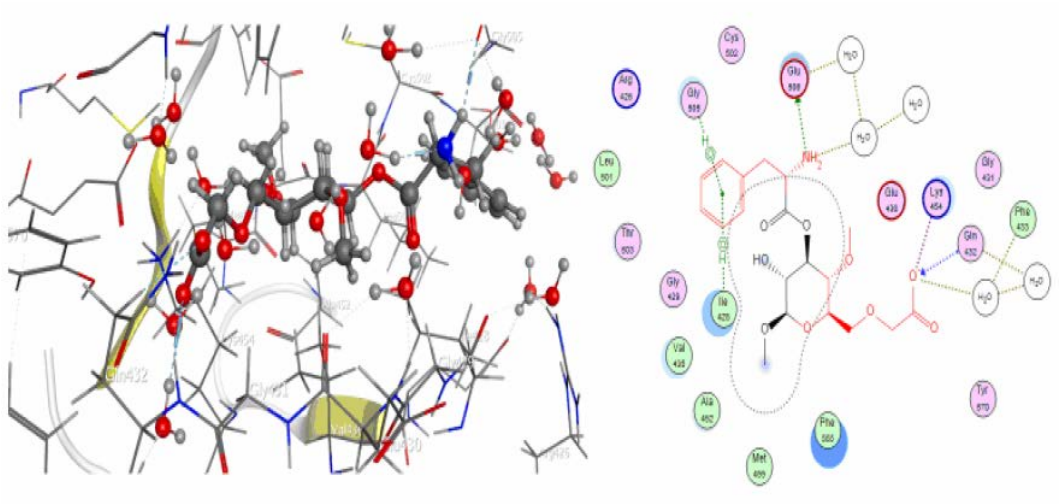

Figure 7. CMC-L-Phe Docked into the active site of FAK, using MOE tool, H-bonds are in blue

CONCLUSIONS

The synthesized ligand derived from bagasse-based CMC with amino acid (L-Phe) was confirmed by different spectral analyses. The experimental results were supported with DFT quantum calculations. Full optimization geometry of the molecule, vibrational spectra, NBO, FMO, thermodynamic parameters, and ESP were calculated. The global and local reactivity: Fukui function index, local electrophilicity and softness were performed, which to be a helpful tool to predict a possible explanation for chemical reactivity of ligand. The BDE values for H gaining showed that the investigated molecule is stable biomolecule against degradation process, which prevent the autoxidation mechanism. Furthermore, the pharma kinetic characters proved the investigarted bioactive compound has low toxic effect and has promising oral bioavailability. The docking study is showed that, the ligand binds at the active site with strong hydrogen bond with catalytic amino, which obeyed with experimental data.

ACKNOWLEDGEMENTS

The authors thank the National Research Centre, ARST, Egypt for funding this work, which regards one deliverable article from Ph. D. thesis of Mohamed S. Hasanin. All other authors are supervisors of this thesis.

REFERENCES

1. El-Saied H, Basta AH, Barsoum BN, El.berry MM. Cellulose membranes for reverse osmosis, Part I. RO cellulose acetate membranes including a composite with polypropylene. Desalination 2003;159: 171-181. https://doi.org/10.1016/S0011-9164(03)90069-5
2. El-Saied H, Abdel-Hadi AK, Hosny WM, Basta AH. Metal chelates with some cellulose derivatives. Part I. Preparation and characterization of chromium (III)–carboxymethyl cellulose complexes. Polymer International 1994;35(1):27-33. https://doi.org/10.1002/pi.1994.210350102
3. Abdel- Hadi AK, Hosny WM, Basta AH, El- Saied H. Metal chelates with some cellulose derivatives. Pt.II-Preparation and characterization of Co(II) - CMC complexes. Polymer Plastic Technology and Engineering 1994;33:781-791. https://doi.org/10.1080/03602559408013108
4. Basta AH, El-Saied H. New approach for utilization of cellulose derivatives metal complexes in preparation of durable and permanent colored papers. Carbohydrate Polymers 2008;74(2):301-308. https://doi.org/10.1016/j.carbpol.2008.02.021
5. Wang Y, Xiong Y, Wang J, Zhang X, Cellulose carbon xerogel supported double-perovskite nanoparticles as aversatile and efficient catalyst for the degradation of humic acid under microwave irradiation. Catalysis Communications 2017;90:14-18. https://doi.org/10.1016/j.catcom.2016.11.010
6. Entcheva E, Bien H, Yin L, Chung CY, Farrell M, Kostov Y. Functional cardiac cell constructs on cellulose-based scaffolding. Biomaterials 2004;25:5753-5762. https://doi.org/10.1016/j.biomaterials.2004.01.024
7. Xing Q, Zhao F, Chen S, McNamara J, DeCoster MA, Lvov YM. Porous biocompatible three-dimensional scaffolds of cellulose microfiber/gelatin composites for cell culture". Acta Materials. 2010;6:2132-2139. https://doi.org/10.1016/j.actbio.2009.12.036

8. Fukuya MN, Senoo K, Kotera M, Yoshimoto M, Sakata O. Enhanced oxygen barrier property of poly(ethylene oxide) films crystallite-oriented by adding cellulose single nanofibers. Polymers 2014;55:5843-5846. https://doi.org/10.1016/j.polymer.2014.09.003
9. Ernsting MJ, Murakami M, Undzys E, Aman A, Press B, Li S-D, J. A docetaxel-carboxymethylcellulose nanoparticle outperforms the approved taxanenanoformulation, Abraxane, in mouse tumor models with significan control of metastases, Control. Release. 2012;162:575-581. https://doi.org/10.1016/j.jconrel.2012.07.043
10. Niazi SK., "Handbook of Pharmaceutical Manufacturing Formulations", 2nd edn. CRC Press 2009. https://doi.org/10.1016/0378-5173(87)90196-7
11. Ranga Rao, KV, Padmalatha Devi K, Buri P. Cellulose matrices for zero order release of soluble drugs. Drug Development and Industrial Pharmacy 1998;14(15–17):2299-2320..
12. Baveja SK, Ranga Rao KV, Padmalatha. K. Zero-order release hydrophilic matrix tablets of [beta]-adrenergic blockers. International Journal of Pharmacy and Pharmaceutical 1987;39:39-45.
13. Valgas C, Machado de Souza S, Smânia EFA, Smânia JrA, Screening Method to Determine Antibacterial Activity of Natural Products. Brazilian Journal of Microbiology 2007;38:369-380. https://doi.org/10.1590/S1517-83822007000200034
14. Sudarsan S, Franklin D.S, Sakthivel, M. Non toxic, Antibacterial, Biodegradable Hydrogels with pH-Stimuli Sensitivity: Investigation of Swelling Parameters, Carbohydrate. Polymers 2016;148:206-215. https://doi.org/10.1016/j.carbpol.2016.04.060
15. Balouiri M, Sadiki M, Ibnsouda SK. Methods for In vitro Evaluating Antimicrobial Activity: A Review Journal of Pharmaceutical Analysis 2016;6:71-79. https://doi.org/10.1016/j.jpha.2015.11.005
16. Van de Loosdrecht AA, Beelen RHJ, Ossenkoppele GJ, Broekhoven MG, Langenhuijsen MMAC. A tetrazolium-based colorimetric MTT assay to quantitate human monocyte mediated cytotoxicity against leukemic cells from cell lines and patients with acute myeloid leukemia. J. Immunolog. Methods 1994;174:311-320. https://doi.org/10.1016/0022-1759(94)90034-5
17. Gera L, Chan DC, Simkeviciene V, Bunn, Jr. PA, Stewar JM. The Proceedings of the 20th American Peptide Symposium 465. 2009. https://doi.org/10.1007/978-0-387-73657-0_200
18. Li H, et al. TarFisDock: a web server for identifying drug targets with docking approach". Nucleic Acids Res. 2006;34:W219-W224. https://doi.org/10.1093/nar/gkl114
19. Wang L, et al. TargetHunter: an in silico target identification tool for predicting therapeutic potential of small organic molecules based on chemogenomic database. AAPS journal. 2013;15:395-406. https://doi.org/10.1208/s12248-012-9449-z
20. Keiser, MJ, et al. Relating protein pharmacology by ligand chemistry. Nature biotechnology 2007;25:197-206. https://doi.org/10.1038/nbt1284
21. Keiser MJ, et al. Predicting new molecular targets for known drugs". Nature 2009;462:175-181. https://doi.org/10.1038/nature08506
22. Gong J, et al. ChemMapper: a versatile web server for exploring pharmacology and chemicalstructure association based on molecular 3D similarity method. Bioinformatics 2013;29:1827-1829. https://doi.org/10.1093/bioinformatics/btt270
23. Liu X, Vogt I, Haque T, Campillos M, HitPick: a web server for hit identification and target prediction of chemical screenings". Bioinforatics 2013;btt303. https://doi.org/10.1093/bioinformatics/btt303
24. Lounkine E, et al. Large-scale prediction and testing of drug activity on side-effect targets. Nature 2012;486:361-367. https://doi.org/10.1038/nature11159
25. Akansu AN, Agirman-TosunH. Generalized Discrete Fourier Transform With Nonlinear Phase. IEEE Transactions on Signal Processing Sep 2010;58(9):4547-4556,
26. Benet LZ. Pharmacokinetic parameters which are necessary to define a drug substance? European Journal of Respiratory Diseases. Supplement 1984;134:45-61. https://doi.org/10.1109/TSP.2010.2050882
27. Zhou SH, Hong Y, Fang GJ. Preparation, characterization and anticancereffect of chitosan nanoparticles. CRTE J. 2007;11(48):9688–9691. https://doi.org/10.1021/bm0502258
28. Karagozlu MZ, Karadeniz F, Kong CS, Kim SK. Aminoethylated chitooligomers and their apoptotic activity on AGS human cancer cells. Carbohdrate Polymers 2012;87:1383-1389. https://doi.org/10.1016/j.carbpol.2011.09.034
29. Basta AH, El-Saied H, El-Deftar M, El-Henawy AA, El-Sheikh HH, Hasanin MS. Properties of modified carboxymethyl cellulose and its use as bioactive compound. Carbohydrate Polymers 2016;153:641-651. https://doi.org/10.1016/j.carbpol.2016.07.051
30. Martinez AGLJ, Marco F. Friedl?nder reaction on 2-Amino-3-cyano-4H-pyrans: synthesis of derivatives of 4H-Pyran [2,3-b] quinoline, new tacrine analogues. Bioorganic and Medical Chemistry Letters 1997;7:3165-3170. https://doi.org/10.1016/S0960-894X(97)10165-2
31. Gaussian 09, Revision D.01, M.J. Frisch, G.W. Trucks, H.B. Schlegel, G.E. Scuseria, M.A. Robb, J.R. Cheeseman, G. Scalmani, V. Barone, B. Mennucci, G.A. Petersson, H. Nakatsuji, M. Caricato, X. Li, H.P.

Hratchian, A.F. Izmaylov, J. Bloino, G. Zheng, J.L. Sonnenberg, M. Hada, M. Ehara, K. Toyota, R. Fukuda, J.Hasegawa, M. Ishida, T. Nakajima, Y. Honda, O. Kitao, H. Nakai, T. Vreven, J.A. Montgomery, Jr., J.E. Peralta, F. Ogliaro, M. Bearpark, J.J. Heyd, E. Brothers, K.N.Kudin, V.N. Staroverov, T. Keith, R. Kobayashi, J. Normand, K. Raghavachari, A. Rendell, J.C. Burant, S.S. Iyengar, J. Tomasi, M. Cossi, N. Rega, J.M. Millam, M. Klene, J.E. Knox, J.B. Cross, V. Bakken, C. Adamo, J. Jaramillo, R. Gomperts, R.E. Stratmann, O. Yazyev, A.J. Austin, R. Cammi, C. Pomelli, J.W. Ochterski, R.L. Martin, K. Morokuma, V.G. Zakrzewski, G.A. Voth, P. Salvador, J.J. Dannenberg, S. Dapprich, A.D. Daniels, O. Farkas, J.B. Foresman, J.V. Ortiz, J. Cioslowski, D.J.Fox, Gaussian, Inc., Wallingford CT, 2013.

32. Molecular Operating Environment (MOE), 2013.08; Chemical Computing Group ULC, 1010 handbook St. West, Suite 910, Montreal, QC, Canada, H3A 2R7, 2017.
33. Parr RG, Chattaraj PK. Principle of maximum hardness. Journal of American Chemical Society 1991;113:1854-1855. https://doi.org/10.1021/ja00005a072
34. Parr RG, Szentpaly LV, Liu S. Electrophilicity Index. Journal of American Chemical Society 1999;121:1922-1924. https://doi.org/10.1021/ja983494x
35. Lamaka SV, Zheludkevich ML,. Yasakau KA, Serra R, Poznyak SK, Ferreira MGS. Nanoporous titania interlayer as reservoir of corrosion inhibitors for coatings with self-healing ability. Progress in Organic Coating 2007;58:127-135. https://doi.org/10.1016/j.porgcoat.2006.08.029
36. Mendoza-Huizar LH, Rios-Reyes CH. Chemical Reactivity of Atrazine Employing the Fukui Function. Journal of the Mexican Chemical Society 2011;55(3):142-147. ISSN 1870-249X
37. Komorowski L, Lipin´ski J, Szarek P, Ordon P. Conceptual DFT analysis of the fragility spectra of atoms along the minimum energy reaction coordinate. Journal of Chemical Physics 2011;135:014109. https://doi.org/10.1063/1.3603449
38. Eddy NO, Ebenso EE, Ibok UJ, Akpan EE. Experimental and Computational Chemistry studies on the inhibition of the Corrosion of Mild Steel in H2SO4by (2s,5s,6r)-6-(2-(aminomethyl)-5-(3-(2-chlorophenyl)isoxazol-5-yl)benzamido)-3,3-dimethyl-7-oxo-4-thia-1-azabicyclo[3.2.0]heptane-2-carboxylic acid. International Journal of Electrochemical Science 2011;6:4296-4315. Retrieved from www.electrochemsci.org/papers/vol6/6094296.pdf
39. Chattaraj PK, Giri S. Stability, Reactivity, and Aromaticity of Compounds of a Multivalent Superatom. Journal of Physical Chemistry A 2007;111:1116-1121. https://doi.org/10.1021/jp0760758
40. Chermette H. Chemical reactivity indexes in density functional theory. Journal of Computational Chemistry 1999;20:129-154. https://doi.org/10.1002/(SICI)1096-987X(19990115)20:1<129::AID-JCC13>3.0.CO;2-A
41. Langenaeker W, De Proft F. Geerlings P. Electron Correlation Effects on Fukui Functions. Journal of Molecular Structure (Theochem) 1996;362:171-175. https://doi.org/10.1016/0166-1280(95)04399-3
42. Roy RK, De Proft F, Geerlings P. Reactivity and Stability of Aromatic Carbonyl Compounds Using Density. Functional Theory - Based Local and Global. Journal of Physical Chemistry A 1998;102:7035-7040. https://doi.org/10.1021/jp9815661
43. Rauk A. Orbital Interaction Theory of Organic Chemistry, 2nd ed., Wiley Interscience, New York 2001:86–136. ISBN: 978-0-471-35833-6
44. Streitwieser A Jr. Molecular Orbital Theory for Organic Chemists, Wiley New York. 1961. https://doi.org/10.1002/ijch.196300023
45. Fleming I. (Frontier Orbitals and Organic Chemical Reactions), John Wiley and Sons, Academic Press, New York 1976. https://doi.org/10.1002/nadc.19770250113
46. Rosenfeld IL. Corrosion Inhibitors, McGraw-Hill, New York. 1981. ISBN:0070541701 9780070541702
47. Tang LB, Mu GN, Liu GH. The Effect of Neutral Red on the Corrosion Inhibition of Cold Rolled Steel in 1.0 M Hydrochloric Acid. Corrosion. Corrosion Science 2003;45:2251-2262. https://doi.org/10.1016/S0010-938X(03)00046-5
48. Manjula P, Manonmani S, Jayaram P, Rajendran S. Anti-Corros. Methods Mater. 2001;48:319-324.
49. Hegazy MA, Hasan AM, Emara MM, Bakr MF, Youssef AH. Evaluating four synthesized Schiff bases as corrosion inhibitors on the carbon steel in 1 M hydrochloric acid. Corrosion Science 2012;65:67- 76. https://doi.org/10.1016/j.corsci.2012.08.005
50. Ayres W, Parr RG. Variational Principles for Describing Chemical Reactions: The Fukui Function and Chemical Hardness Revisited. Journal of American Chemical Society 2000;122:2010-2018. https://doi.org/10.1021/ja9924039
51. Clark DE, Pickett SD. Computational methods for the prediction of 'drug-likeness'. Drug Discovery Today 2000;5:49-58. https://doi.org/10.1016/S1359-6446(99)01451-8
52. Zhao Y, Abraham MH, Lee J, Hersey A, Luscombe N, Beck G, Sherborne B, Cooper I. Rate-limited steps of human oral absorption and QSAR studies. Pharmaceutical Research 2002;19:1446-1457. https://doi.org/10.1023/A:1020444330011

53. Wildman SA, Crippen GM. Prediction of physicochemical parameters by atomic contributions. Journal of Chemical Information and computation Science 1999;39:868-873. https://doi.org/10.1021/ci9903071
54. Pharma Algorithms. Web Edition. 2009;5.
55. Moda TL, Torres LG, Carrara AE, Andricopulo AD. PK/DB: database for pharmacokinetic properties and predictive in silico ADME models. Bioinfomatics 2008;24:2270 -2271. https://doi.org/10.1093/bioinformatics/btn415
56. Schaller MD, Borgman CA, Cobb BS, Vines RR, Reynolds AB, Parsons Proc JT. pp125 FAK a structurally distinctive protein-tyrosine kinase associated with focal adhesions. Proceedings of the National Academy of. Scie Proc Natl Acad Sci U S A. 19nce. USA. 1992;89:5192-5196. https://doi.org/10.1073/pnas.89.11.5192
57. Golubovskaya V, Beviglia L, Xu LH, Earp HS, Crraven R, Cance W. Dual inhibition of focal adhesion kinase and epidermal growth factor receptor pathways cooperatively induces death receptor-mediated apoptosis in human breast cancer cells. Journal of Biological Chemistry 2002;277:38978- 38987. https://doi.org/10.1074/jbc.M205002200
58. Schaller MD. Biochemical signals and biological responses elicited by the focal adhesion kinase, Biochimica et. Biophysica Acta 2001;1540:1-21. https://doi.org/10.1016/S0167-4889(01)00123-9
59. Parsons JTJ. Discovery of FAK Inhibitors Using Structure Based Drug Design. Cell Sci. 2003;116:1409-1416. https://doi.org/10.1242/jcs.00373

SUPPLEMENTARY MATERIAL

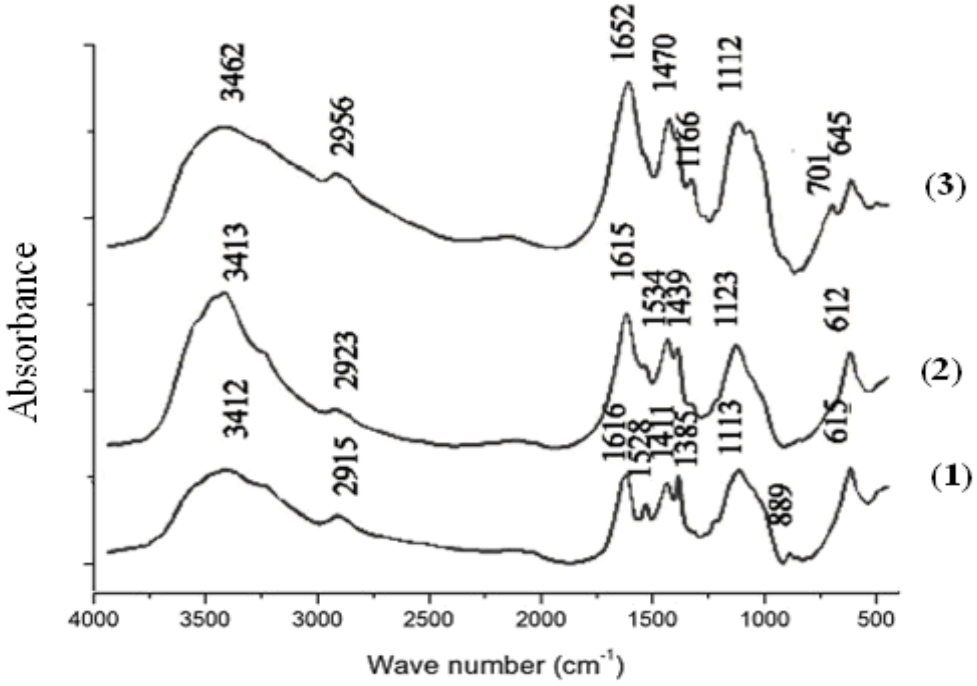

Sup. Fig. 1: FT-IR spectra of bagasse α-cellulose fibers (1) , CMC (2), and conjugated bagasse (3)

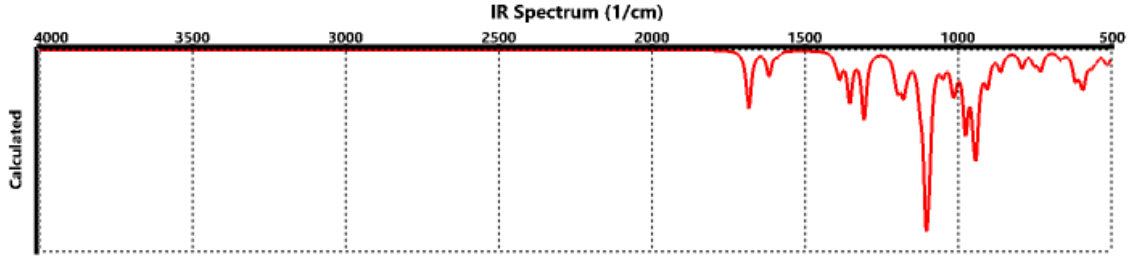

Sup. Fig. 2: calculated vibrational frequencies for the most stable stereoisomer form of the ***CMC-L-Phe*** as calculated by DFT molecular orbital theory with **B3LYP/6-311G*** calculations

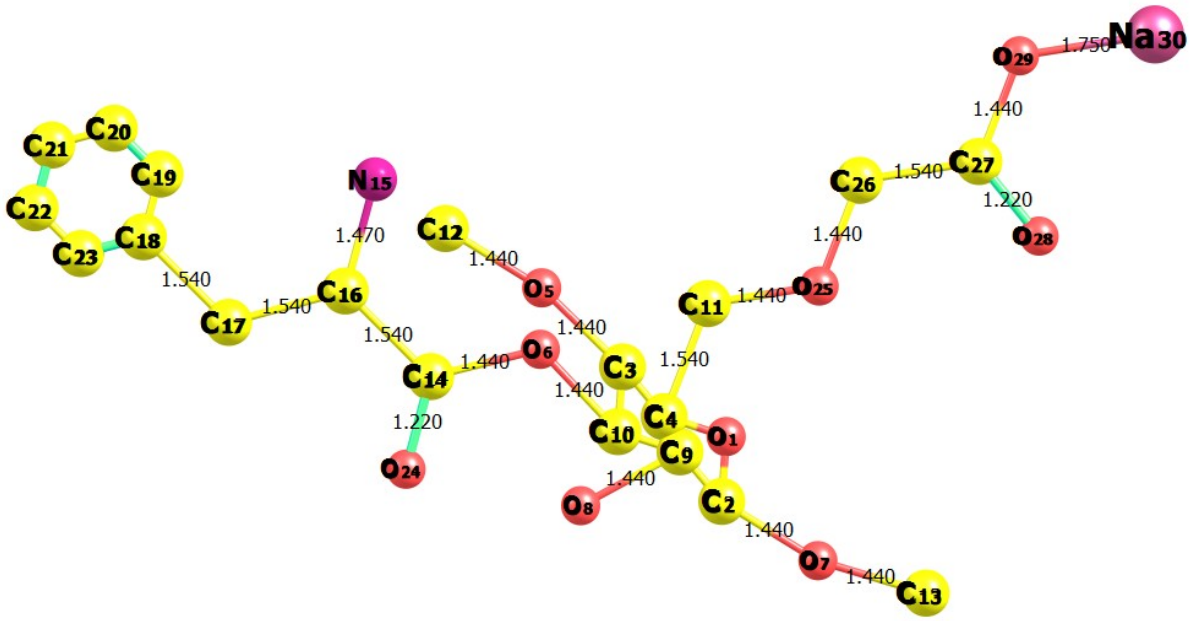

Sup. Fig. 3: bond length ofBall and stick rendering for the **CMC-D-Phe** stereoisomer form of the ligand as calculated by DFT molecular orbital with B3LYP/6-311G* calculations

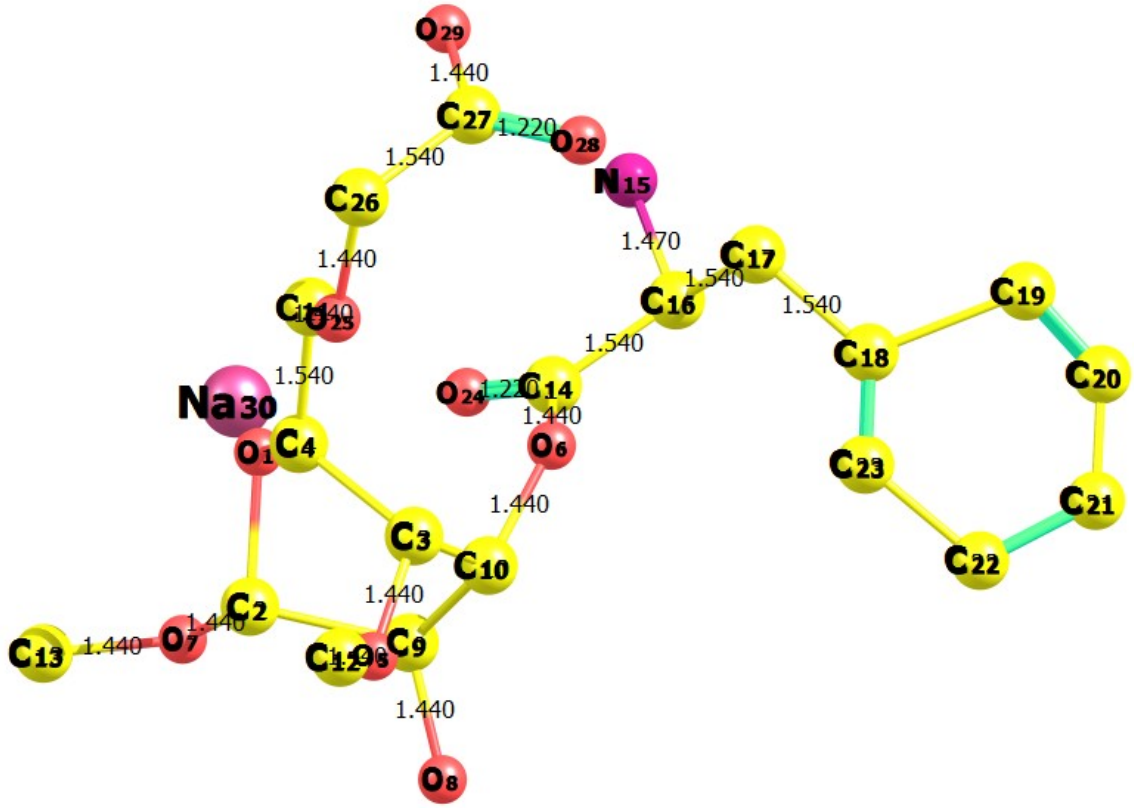

Sup. Fig. 4: Bond length ofBall and stick rendering for the **CMC-L-Phe** stereoisomer form of the ligand as calculated by DFT molecular orbital with B3LYP/6-311G* calculations

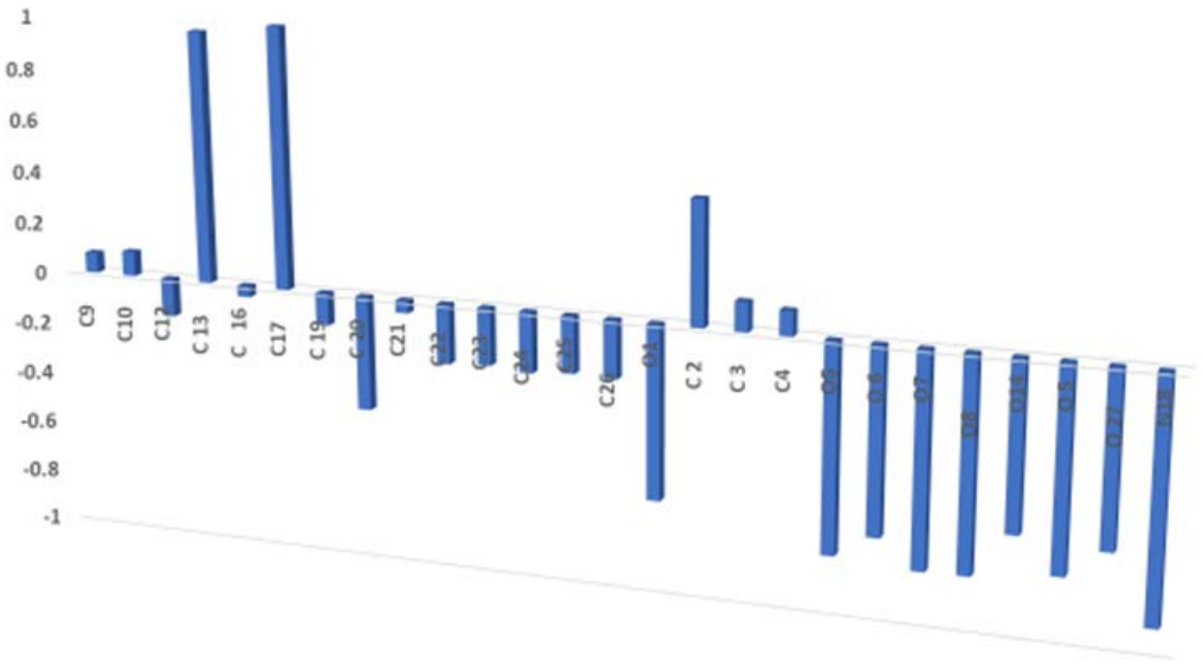

Sup. Fig. 5: Natural bond orbital (NBO) of CMC-L-Phe stereoisomer form of the ligand as calculated by DFT molecular orbital with B3LYP/6-311G* calculations